

Attenuated Response to In Vivo Mechanical Loading in Mice With Conditional Osteoblast Ablation of the Connexin43 Gene (*Gjal*)*

Susan K Grimston,¹ Michael D Brodt,² Matthew J Silva,² and Roberto Civitelli^{1,2}

ABSTRACT:

Introduction: In vitro data suggest that gap junctional intercellular communication mediated by connexin43 (Cx43) plays an important role in bone cell response to mechanical stimulation. We tested this hypothesis in vivo in a model of genetic deficiency of the Cx43 gene (*Gjal*).

Materials and Methods: Four-month-old female mice with a conditional *Gjal* ablation in osteoblasts (*ColCre;Gjal*^{-flox}), as well as wildtype (*Gjal*^{+flox}) and heterozygous equivalent (*Gjal*^{-flox}) littermates (eight per genotype), were subjected to a three-point bending protocol for 5 d/wk for 2 wk. Microstructural parameters and dynamic indices of bone formation were estimated on sections of loaded and control contralateral tibias.

Results: *ColCre;Gjal*^{-flox} mice had significantly thinner cortices, but larger marrow area and total cross-sectional area in the tibial diaphysis, compared with the other groups. The *ColCre;Gjal*^{-flox} mice needed ~40% more force to generate the required endocortical strain. In *Gjal*^{+flox} mice, the loading regimen produced abundant double calcein labels at the endocortical surface, whereas predominantly single labels were seen in *ColCre;Gjal*^{-flox} mice. Accordingly, mineral apposition rate and bone formation rate were significantly lower (54.8% and 50.2%, respectively) in *ColCre;Gjal*^{-flox} relative to *Gjal*^{+flox} mice. Intermediate values were found in *Gjal*^{-flox} mice.

Conclusions: *Gja* deficiency results in thinner but larger tibial diaphyses, resembling changes occurring with aging, and it attenuates the anabolic response to in vivo mechanical loading. Thus, Cx43 plays an instrumental role in this adaptive response to physical stimuli.

J Bone Miner Res 2008;23:879–886. Published online on February 18, 2008; doi: 10.1359/JBMR.080222

Key words: connexin43, mechanical load, bone morphology

INTRODUCTION

GAP JUNCTIONS CONSIST of intercellular channels that provide aqueous continuity between adjacent cells, thus allowing the diffusion of small molecules and ions from cell to cell. Gap junctions are composed of a hexameric array of protein subunits, connexins, which form a transmembrane channel, called a connexon. When two connexons on adjacent cells dock to each other, they form a transcellular gap junction channel.^(1,2) The most abundant connexin found in bone is connexin43 (Cx43),^(3–5) although connexin45 (Cx45) and connexin46 are also present.^(3,6) The importance of Cx43 in the skeletal system was shown by the skeletal developmental abnormalities and osteoblast dysfunction in mice with a null mutation of the *Cx43* gene (*Gjal*),⁽⁷⁾ and it is further underscored by the skeletal malformations featuring oculodentodigital dysplasia, a human

disease caused by loss-of-function mutations of *Gjal*.^(8,9) Similar malformations have also been reported in mice heterozygous for mutations of *Gjal* that phenocopy oculodentodigital dysplasia.^(10,11)

In vitro studies have shown that Cx43 is involved in mechanotransduction. Inhibition of gap junctional intercellular communication (GJIC) and/or *Gjal* gene expression hinders osteoblast responses to fluid flow^(12,13) and mechanically induced calcium waves.⁽¹⁴⁾ Furthermore, Cx43 abundance and *Gjal* gene expression are upregulated by different types of mechanical load.^(15,16) However, translation of these findings to in vivo settings has thus far been limited by the lack of suitable models, since homozygous *Gjal*-null mice die shortly after birth because of major cardiovascular malformations.^(17,18)

To overcome these limitations, we recently developed mice in which the *Gjal* gene is deleted selectively in osteoblasts and osteocytes using the *Cre/loxP* approach.⁽¹⁹⁾ In this model, Cre-induced gene recombination is driven by a fragment of the $\alpha_1(I)$ collagen promoter, leading to gene ablation specifically in differentiated osteoblasts and osteo-

*Presented in part at the 29th annual meeting of the American Society for Bone and Mineral Research, September 16–19, 2007, Honolulu, Hawaii, USA.

The authors state that they have no conflicts of interest.

¹Division of Bone and Mineral Disease, Department of Internal Medicine, Washington University School of Medicine, St Louis, Missouri, USA; ²Department of Orthopaedic Surgery, Washington University School of Medicine, St Louis, Missouri, USA.

cytes.⁽²⁰⁾ These mice are osteopenic and exhibit an attenuated response to the anabolic effect of intermittent PTH administration, the consequence of a failure to increase osteoblast activity on hormonal stimulation despite an increase in osteoblast number.⁽²⁰⁾ Based on this remarkable finding, we reasoned that in vivo anabolic responses to other stimuli, such as mechanical loading might also be dependent, at least in part, on Cx43, a hypothesis also emerging from the existing body of in vitro data. To test this hypothesis, we used a three-point bending model of mechanical loading, which stimulates new bone formation on the endocortical surface in areas subject to physical strain. We found that mice with conditional inactivation of *Gjal* in osteoblasts and osteocytes exhibit attenuated osteoblast activation in response to mechanical loading, relative to their wildtype equivalent littermates, showing that Cx43 is involved in the responsiveness to mechanical signals that are anabolic to bone. These observations generalize the role of Cx43 in adaptive responses that require osteoblast activation.

MATERIALS AND METHODS

Transgenic mice

The mouse model used in these studies has already been described.^(19,20) Briefly, mice harboring a floxed *Gjal* allele (*Gjal^{fllox}*) were mated with mice expressing Cre under control of a 2.3-kb $\alpha_1(I)$ collagen promoter fragment (*ColCre*) so that Cre-mediated recombination replaces the entire *Gjal* reading frame with a *lacZ* reporter cassette. Homozygous *Gjal^{fllox/fllox}* mice were mated with *ColCre* mice also carrying a *Gjal*-null allele (*ColCre;Gjal^{+/-}*) to generate, in approximately equal numbers, the three genotypes of interest: *ColCre;Gjal^{-fllox}* (conditional knockout [cKO]), *Gjal^{+fllox}* (wildtype equivalent [WT]), and *Gjal^{-fllox}* (heterozygous equivalent [Het]), as well as *ColCre;Gjal^{+fllox}* (conditional heterozygous; data not analyzed). All mouse lines were produced in a mixed C57BL/6-C129/J background. Mice were fed regular chow and housed communally in a room maintained at a constant temperature (25°C) on a 12-h light/dark cycle. Although dental abnormalities are present in *Gjal* mutant mice resembling the human disease oculodentodigital dysplasia,⁽¹⁰⁾ no such abnormalities were observed in *ColCre;Gjal^{-fllox}* mice. Indeed, average food intake was similar in cKO and WT mice (0.22 ± 0.01 versus 0.25 ± 0.02 g/g/d, respectively).

Genotyping was performed by PCR on genomic DNA extracted from mouse tails, using primers and conditions previously described.⁽²⁰⁾ To further confirm Cre-mediated DNA recombination, the deleted *Gjal* allele was directly identified in whole bone extracts in all cKO mice used in the study. To this end, DNA was extracted from the left femur, after tissue pulverization in liquid nitrogen using a Bessman Tissue Pulverizer (Fisher), by applying an adaptation of the HotSHOT method.⁽²¹⁾ For these studies, only 4-mo-old female mice were used. Twenty-four mice (8 per genotype) were used for the bone morphometry analysis, 17 mice were used in the calibration phase of the study, and 24 mice were used for the in vivo loading phase. All animals

continued unrestricted weight-bearing activity between loading sessions. There were no observable differences in morphology between the calibration mice and the in vivo loaded mice or in activity levels among genotypes during the loading phase. All procedures were approved by the Animal Studies Committee of Washington University in St Louis.

BMD

Region-specific BMD was measured both at baseline (preload) and at the end of the 2-wk loading period (postload) by DXA (PIXImus Lunar-GE), as described previously.⁽²⁰⁾ Regions of interest were identified in a 0.1-cm² area corresponding to the midpoint between the tibiofibular junction (TFJ) and proximal tibial metaphysis. The region of interest included only the tibial diaphysis and therefore represents cortical bone only. However, postload measurements also included the new periosteal woven bone formed in response to load. Calibration of the DXA was performed daily with a standard phantom as per the manufacturer's instructions. The precision of whole body BMD is 1.34% (CV).⁽²²⁾ All tibial analyses were conducted by a single investigator (SKG). Body weight was measured at the time of BMD testing and also monitored during the in vivo load phase of the study.

Calibration study

Calibration studies were performed on six WT, five Het, and six cKO female mice using a three-point tibial bending model before the in vivo loading, following a method described previously.⁽²³⁾ Briefly, after death, the right hind limb was dissected minimally for strain gauge placement. Muscles were retracted to expose the antero-medial surface of the right tibia. Tensile strains are generated on this surface by the bending protocol. A 1-mm-long strain gauge (Tokyo Sokki Kenkyujo Co.) was applied to the exposed surface of the bone, midway between the TFJ and the proximal tibial metaphysis. Mice were positioned in a servohydraulic materials testing machine (Instron; Dynamight) such that the central loading point was approximately equidistant from the distal TFJ and the knee joint. The two supports were 11 mm apart.

After application of a 0.5 N compressive preload, a trapezoidal waveform was applied up to the target peak force with a 10-s interval between each of eight loading cycles. Strains were recorded through a signal conditioning amplifier system (SCX1-1001; National Instruments). Peak forces of 4, 8, 12, 16, 20, and 24 N were applied with a 160-s recovery interval between each set of eight cycles. Peak strains were determined for cycles 4–8, and the average was computed. The region of the bone at the gauge site, with the strain gauge attached, was scanned using μ CT (μ CT 40; Scanco, Basserdorf, Switzerland) to assess the location of the strain gauge and the relative distance from the centroid to the periosteal and endocortical surfaces. Force-periosteal strain calibration curves were generated for each genotype. Endocortical strains were estimated from the periosteal strain data and the μ CT-based geometry using simple beam theory, an approach that has been validated by finite ele-

TABLE 1. MICROSTRUCTURAL INDICES OF TIBIAL CORTICAL BONE IN THE THREE GENOTYPES

Index	WT	Het	cKO
Cortical thickness (mm)	0.159 ± 0.007	0.147 ± 0.041*	0.130 ± 0.056*
Total area (mm ²)	1.23 ± 0.09	1.62 ± 0.13*	1.55 ± 0.12*
Marrow area (mm ²)	0.53 ± 0.15	0.79 ± 0.13*	0.77 ± 0.12*
Cortical area (mm ²)	0.70 ± 0.15	0.83 ± 0.05*	0.78 ± 0.08
Moment of inertia (mm ⁴)	0.128 ± 0.054	0.147 ± 0.038	0.130 ± 0.059

* $p < 0.05$ vs. WT; $n = 8$ for all groups.

ment analysis.⁽²³⁾ From the average force-endocortical strain curves, the forces necessary to produce 1600 $\mu\epsilon$ at the anterior-lateral endocortical surface of the tibia (site of highest endocortical strain) for each genotype were determined and used in the in vivo study.

In vivo loading study

Mice were anesthetized with 1–3% isoflurane and positioned in the loading apparatus as for the strain gauge study. The relevant compressive load was applied on the tibia as specified by the calibration study, such that the lateral surface of the tibia was in compression and the medial surface in tension. The left leg was not loaded and served as a contralateral control. The load/unload time was 0.5 s, followed by a 10-s rest interval.⁽²⁴⁾ Sixty cycles were applied in one bout each day, 5 d/wk for 2 wk, a time period shown to be adequate for stimulating an acute bone anabolic response in mice⁽²⁵⁾ and rats.^(26,27) Animals were given buprenorphine (0.1 mg/kg, SC) immediately after loading. There were no observable differences in activity levels after recovery from anesthesia among groups. Mice were injected with calcein (15 mg/kg, IP; Sigma-Aldrich, St Louis, MO, USA) on days 5 and 12 and killed on day 15.

After death, right and left tibias were dissected and cleaned of all connective tissue. The left femur was cleaned on ice and flash frozen before being stored at -80°C until DNA extraction. The right and left tibias and the right femur were stored in 10% buffered formalin for up to 24 h and placed in 70% ethyl alcohol at 4°C before embedding in methyl methacrylate for histological analysis.

Bone microstructure

Left and right tibias were stabilized in 1.5% agarose gel, and a 1-mm-thick region along the length of the tibia, equidistant from the TFJ and the proximal tibial metaphysis was scanned at 16- μm voxel resolution (μCT 40; Scanco Medical AG). Total tissue cross-sectional area (Tt.Ar.) and marrow area (Ma.Ar) were measured. Cortical area (Ct.Ar) was calculated as the difference between total cross-sectional and marrow area (Tt.Ar. – Ma.Ar), and moment of inertia was calculated relative to the axis of bending (anterior-posterior). Mean cortical thickness (Ct.Th.) was determined from the left tibia by measuring the cortical width at four different locations and taking the average value. All measured and derived variables were expressed according to the standard nomenclature.⁽²⁸⁾

Bone histomorphometry

Right and left tibias were embedded in methyl methacrylate using the method described previously.⁽²⁰⁾ Quantita-

tive histomorphometry was performed on 80- μm transverse sections using the OsteoMeasure software program (Osteometrix) in an epifluorescent microscope system, as detailed elsewhere.⁽²²⁾ Measurements were taken on three consecutive sections (80 μm) at the loaded site per tibia. Similar sections were taken and measured from the contralateral tibia. Single (sLS/BS) and double (dLS/BS) labeled surface, mineralizing surface (MS), interlabel thickness (Ir.L.Th.), and mineral apposition rate (Ir.L.Th/Ir.L.t = MAR) were measured and calculated. The interlabel time (Ir.L.t.) was 7 days. Bone formation rate with bone surface as the referent (BFR/BS) was calculated as (MAR \times Md.S/BS \times 3.65; $\mu\text{m}^3/\mu\text{m}^2/\text{yr}$). Only labels on the endocortical surface were measured because this was our primary site of interest. Relative loading effect was calculated as (Loaded–Contralateral) for MS, MAR, and BFR/BS.⁽²⁹⁾

Statistical analyses

ANOVA was used to assess differences among genotypes for each of the variables studied. Posthoc Bonferroni's multiple comparison procedure was used to determine which values were significantly different. Where appropriate, an unpaired t -test was used for group comparisons. A paired t -test was used for comparisons of the loaded and contralateral tibias. Data were analyzed using Statgraphics Plus 3.0 (Manugistic) with the level of significance for comparison set at $p < 0.05$. All data are expressed as the mean \pm SD unless otherwise noted.

RESULTS

Geometric properties of *Gja1* cKO mice

Microstructural analysis by μCT showed that tibias from conditional *Gja1* ablated mice (*ColCre;Gja1^{-flox}*, cKO) had significantly thinner cortices, greater total tissue cross-sectional area, and greater marrow area than their wildtype (*Gja1^{+flox}*, WT) littermates (Table 1). In heterozygous equivalent mice (*Gja1^{-flox}*, Het), these structural parameters of cortical bone were closer to those observed in cKO mice, although cortical thickness was intermediate between the two other genotypes (Table 1). These differences reflect a thinner, larger bone in cKO (and to a lesser extent the Het) relative to WT mice, as shown in the examples of Fig. 1. However, despite these structural differences, there were no differences among groups for moment of inertia (Table 1).

Strain gauges were applied to determine the force-strain curves for each genotype and thus calculate the appropriate load that would produce an equal endocortical strain in

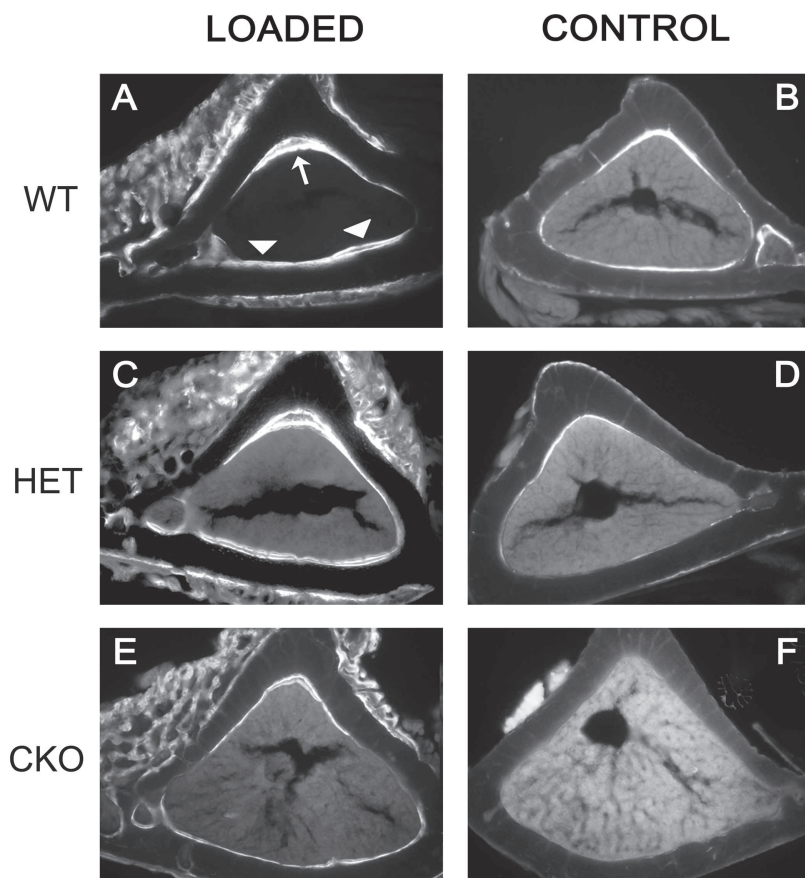


FIG. 1. Attenuated mechanical stimulation of new bone formation in mice with conditional ablation of *Gja1*. Fluorescence micrographs of calcein-labeled tibial mid-diaphysis cross-sections corresponding to the area subjected to mechanical load (A, C, and E) and to the same area in unloaded, contralateral tibias (B, D, and F). Note also the thinner tibial cortex and larger marrow area of the CKO mice (E and F) compared with that of the WT (A and B). (A) Double calcein labels are present in the endocortical surface of loaded bones of wildtype *Gja1*^{+/*fl*ox} mice (WT) at the apex (large arrow) and at the opposite endocortical surface (arrowheads), corresponding to the areas of maximum endocortical compression and tension, respectively. (C) Double-labeled surfaces are also seen in *Gja1*^{-/*fl*ox} tibias (HET), whereas (E) predominantly single labels are present in *ColCre;Gja1*^{-/*fl*ox} (CKO) tibial sections. (B, D, and F) Primarily single labels are seen in control, unloaded bones. Note also the periosteal woven bone around the area of loading, evident for each genotype.

mice of the different genotypes. Strain increased linearly with applied force for each genotype. The slopes of the regression lines for endocortical strain versus load differed between genotypes, with WT mice having a steeper slope, indicating that a lower force level is needed in WT than cKO mice to generate the same endocortical strain. Based on these results, we applied 8.7N, 14.2N, and 12.2N to WT, Het, and cKO mice, respectively, to generate an estimated 1600 $\mu\epsilon$ at the endocortical surface in the loading experiments. The average periosteal strains corresponding to these *in vivo* loading loads were 3774 (WT), 3913 (Het), and 4665 $\mu\epsilon$ (cKO).

Response to *in vivo* loading

There were no significant changes in weight through the course of the experiment either within or between groups (Table 2). Furthermore, BMD of the tibial diaphysis did not differ among genotypes before skeletal load was applied, and it significantly increased in all groups after loading (Table 3). However, tibial BMD was lower in cKO relative to WT mice after loading, and the difference barely missed the significance level ($p = 0.06$; Fig. 2A). Similarly, the differences in Ct.Ar. between loaded and contralateral tibias, analyzed by μ CT in the same region included in the DXA scans, were lower in the cKO compared with the other genotypes, but the differences were not significant (Fig. 2B). Application of the three-point bending loading protocol also resulted in formation of exuberant woven

TABLE 2. BODY WEIGHT AT BASELINE AND AFTER LOADING IN THE THREE GENOTYPES

Body weight (g)	WT	Het	cKO
Before loading	21.4 \pm 1.4	24.0 \pm 3.8	22.1 \pm 1.9
After loading	21.6 \pm 0.9	23.2 \pm 2.5	21.3 \pm 1.7

$n = 8$ for all groups.

bone on the periosteal surface, primarily in the area where the compressive force was applied (Figs. 1A, 1C, and 1E). The structural changes induced by mechanical loading are largely consistent for all parameters studied.

Dynamic histomorphometry showed abundant double calcein labels on the endocortical surface of WT mouse tibias after loading compared with single or no labels in the contralateral control tibias (Figs. 1A and 1B). Less abundant, although evident double labels were also seen in loaded Het tibias, relative to contralateral tibias (Figs. 1C and 1D). In contrast, primarily single calcein labels and few areas of double labels were observed in conditionally deleted *Gja1* mice (Figs. 1E and 1F). Accordingly, parameters of new bone formation (i.e., MAR, BFR, and MS) were significantly higher in WT than in cKO tibias after the 2-wk loading regimen, with Het mice falling somewhat in between the other two groups (Table 3). MAR and BFR in cKO-loaded tibias were 54.8% and 50.2% of WT mice, respectively.

TABLE 3. BONE DENSITY AND DYNAMIC INDICES OF BONE FORMATION IN LOADED AND CONTROL (CONTRALATERAL) TIBIAS IN THE THREE GENOTYPES

Index	Control			Loaded		
	WT	Het	cKO	WT	Het	cKO
BMD (mg/cm ²)	49.3 ± 1.9	52.0 ± 1.9	41.9 ± 2.4	61.8 ± 6.6*	62.6 ± 6.6*	56.9 ± 3.7*
MS (mm)	8.19 ± 3.28	8.52 ± 3.14	13.02 ± 7.59	27.68 ± 6.96*	19.49 ± 8.69*†	19.22 ± 9.02†
MAR (μm/d)	0.613 [‡]	0.518 ± 0.259	0.826 ± 0.273	1.86 ± 0.94	1.86 ± 0.94*	1.02 ± 0.97 [§]
BFR/BS (μm ³ /μm ² /yr)	25.37 [‡]	24.02 ± 3.75	26.29 ± 28.56	207.66 ± 93.37	187.87 ± 142.62*	104.25 ± 111.92†

* $p < 0.05$ vs. control.† $p < 0.05$ vs. WT loaded.N = 3–8, except [‡] n = 2.§ $p < 0.05$ vs. WT and Het loaded.

Dynamic bone formation data were also expressed as the difference between loaded and contralateral (control) tibias to better determine the degree of osteoblast activation in each genotype. Because all the parameters were not statistically different among the three genotype groups in the contralateral tibias, this correction did not substantially change the outcome, resulting in a significantly 50–70% lower MAR, BFR, and MS in loaded cKO relative to WT mice, with intermediate responses observed in Het mice (Figs. 3A–3C).

DISCUSSION

This study showed that deletion of *Gjal* in osteoblasts and osteocytes leads to changes in adult bone morphology and attenuates the bone anabolic response to skeletal mechanical loading. These abnormalities are likely caused by a functional defect in osteoblasts, which fail to increase their response to the mechanical stimulus, thus showing that Cx43 plays a significant role in bone's response to mechanical stimulation.

This analysis showed aspects of the phenotype of cKO mice that had not emerged in our earlier report.⁽²⁰⁾ Cortical bone at the tibial diaphysis of conditionally deleted animals was thinner, but overall cross-sectional size and bone marrow area were larger than in wildtype mice. The resulting expanded bone size together with the thinner cortex may explain why cortical area and BMD were not decreased in cKO mice, although it should be noted that the sensitivity of DXA in estimating BMD in small anatomical areas is very limited. The cortical bone structure of *Gjal*-deficient mice is reminiscent of the chronic adaptive changes seen in human aging, where endocortical resorption is compensated for by periosteal bone apposition, resulting in thinner cortical bone and larger diaphyseal cross-sections.^(30,31) Accordingly, the larger endocortical surface is suggestive of an imbalance between bone formation and resorption at the endocortical surface in cKO mice, perhaps reflecting a reduced activation of bone formation in response to mechanical stimuli. Enlarged cross-section of tibial diaphyses and thinner cortical bone are also evident in *Gjal*^{Jr} mice, which partially phenocopy oculodentodigital dysplasia.⁽¹⁰⁾ It remains to be determined whether these morphological differences represent an age-dependent biomechanical adaptation to the lower whole body bone mass of cKO mice⁽²⁰⁾ or reflect a skeletal developmental anomaly. In any case,

these morphological abnormalities would predict that the moment of inertia is greater in cKO mice. However, the calculated cross-sectional moment of inertia was not significantly different in the mutant relative to WT mice, a finding that is also at odds with the differences in the force-strain relationship between genotypes. These inconsistencies cannot be resolved at the present but may be attributed to the irregular size of the tibial cross-section.

The major finding of this study is the demonstration that mice with *Gjal* ablation in osteoblasts and osteocytes exhibit an attenuated anabolic response to mechanical loading on the tibial endocortical surface. Such a finding is quite consistent with our previous reports of attenuated anabolic response to intermittent PTH administration in the same mouse strain.⁽²⁰⁾ Even in that case, attenuated in vivo bone anabolism was associated with deficient MAR and BFR, despite an increase in osteoblast number, suggesting a functional defect in Cx43-deficient osteoblasts. This study suggests that the functional defects produced by Cx43 deficiency in bone-forming cells are not restricted to hormonal responsiveness but represent a fundamental abnormality that hinders these cells from activating in response to different anabolic stimuli. Also consistent with our previous study on intermittent PTH administration,⁽²⁰⁾ Het mice had a response that generally fell between that of the WT and cKO mice, suggesting a *Gjal* gene dosage effect in response to the mechanical stimulus.

The attenuated response could be either caused by impaired mechanotransduction (i.e., converting the mechanical stimulus into a cellular response) or impaired osteoblast function. It is possible that bone cells transduce the mechanical signal but cannot produce a maximal anabolic response because their ability to form bone depends on Cx43 mediated cell–cell communication. Based on previous data, both mechanisms are possibly involved. It is worth noting that the anabolic response to mechanical loading was attenuated but not abolished in cKO mice, showing either that Cx43 is not absolutely necessary for mechanoresponsiveness in vivo or that compensatory mechanism(s) exist for the absence of Cx43. Osteoblasts express other connexins, particularly Cx45, which does form functional gap junctions with unique biophysical properties.⁽⁶⁾ Although overexpression of Cx45 negatively interferes with Cx43-mediated gap junctional communication,^(32,33) it is possible that Cx45 may provide a partial compensatory mechanism

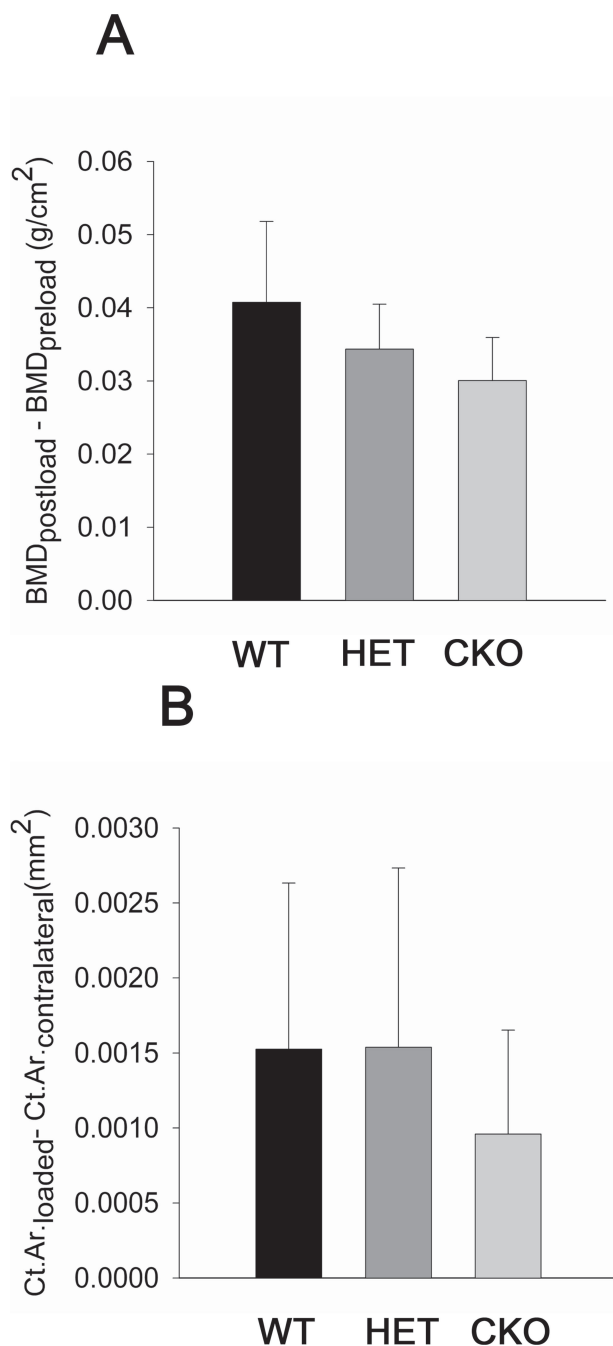


FIG. 2. Relative effect of the loading regimen on BMD and cortical area (Ct.Ar.). BMD is expressed with respect to measures taken before loading (preload), whereas Ct.Ar. is expressed relative to values for the contralateral control tibia. Results for *Gjal*^{+/*flox*} wildtype (WT), *Gjal*^{-/*flox*} heterozygous (HET), and *ColCre;Gjal*^{-/*flox*} conditional knockout (CKO).

in the absence of Cx43, even though Cx45 abundance is not affected in *ColCre;Gjal*^{-/*flox*} mice.⁽²⁰⁾

In addition to activation of endocortical bone formation, there was a robust periosteal response to mechanical loading using the three-point bending protocol in all three genotypes. This may have accounted, in large part, for the increased BMD detected by DXA after loading. However,

this exuberant periosteal new bone formation is likely influenced by periosteal contact pressure in addition to bending strains.⁽³⁴⁾ Nonetheless, we do not believe that the differences in applied force (and therefore pressure) between the genotypes would have contributed to the differences in endocortical bone formation. In other studies, increasing the applied force within the same strain of animal leads to increased endocortical bone formation in rats⁽³⁵⁾ and mice (MJ Silva and MD Brodt, unpublished data, 2005). In addition, periosteal pressure without tibial bending does not stimulate endocortical bone formation even as it stimulates periosteal woven bone.⁽³⁵⁾ Thus, available evidence indicates that the periosteal response does not influence the endocortical response.

Notably, the mice used in this study were generated in a mixed C57BL/6-C129J background, because bone mass and responses to anabolic stimuli are variable among different strains. For example, C57BL/6 mice have low bone mass relative to the C129J strain.⁽³⁶⁾ Interestingly, although C57BL/6J mice have a significantly greater total cortical area and cross-sectional moment of inertia than C3H/HeJ mice, despite a lower bone mass, they exhibit a greater anabolic response to mechanical load than do C3H/HeJ mice.⁽²⁵⁾ Different sensitivities to mechanical load have been repeatedly observed in different mouse strains, and in general, mice with lower bone mass exhibit greater anabolic response to mechanical load than mice of high bone mass.^(25,37,38) It is difficult to compare the degree of responsiveness of our mice with those of other studies because of the mixed background and the different modes of mechanical intervention used.^(25,37) Nonetheless, we were able to see a significant attenuation of new bone formation in response to skeletal mechanical load in *Gjal*-deficient mice. It is reasonable to believe that such defective response might have resulted in significantly smaller cortical bone gains in our genetically deficient animals if the mechanical stimulation was applied for a more prolonged period of time, as suggested by the trends in both cortical area and BMD after 2 wk of load. Alternatively, it could be argued that the response might only be delayed in these cKO mice, based on our previous observation of a delayed osteoblast maturation in vitro.⁽²⁰⁾ A longer period of loading may help resolve this uncertainty, although the larger bones and thinner cortices of *ColCre;Gjal*^{-/*flox*} mice, also observed in another *Gjal* mutant mouse model,⁽¹⁰⁾ would support the hypothesis of inherent defects of adaptive mechanisms rather than a simple delay in response to load.

When testing mechanoresponsiveness in vivo, it is important to apply equivalent levels of stimulus to each group of experimental animals. This is difficult when genetic differences result in different bone sizes, as in our case. The prevailing approach is to adjust the applied force magnitude so that an equivalent peak strain magnitude is applied to each group. This is typically done directly from strain gage data relating force to periosteal strain. However, in our case, we were interested in equating the strain at the endocortical surface, because this was our primary surface of interest in light of confounding effects of contact pressure on periosteal responses in the tibial bending model. Interestingly, the estimated relationships between force and en-

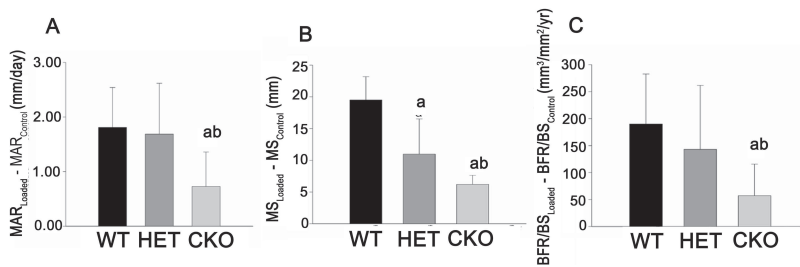


FIG. 3. Effect of mechanical skeletal loading on new bone formation in *Gjal*^{+/flox} wild-type (WT), *Gjal*^{+/flox} heterozygous (HET), and *ColCre;Gjal*^{-flox} conditional knockout (CKO) mice. Data are expressed as the difference between loaded and unloaded tibia for (A) mineral apposition rate (MAR), (B) mineralizing surface (MS), and (C) bone formation rate (BFR/BS) in each genotype. ^a*p* < 0.05 vs. WT; ^b*p* < 0.05 vs. WT and HET.

docortical strain dictated that we apply ~40% greater force magnitude to the genetically deficient animals than to wild-type mice. Thus, the anabolic response was significantly attenuated in conditionally ablated mice despite application of a much higher level of applied force.

The molecular mechanisms underlying bone's response to mechanical load remain to be elucidated. We have previously shown that interference with *Gjal* alters expression of osteoblast genes, particularly $\alpha_1(I)$ collagen, osteocalcin, and bone sialoprotein, the consequence of transcriptional downregulation of specific gene promoter elements through MAP/ERK/PI3 kinase- and protein kinase C-dependent pathways.^(39,40) Because activation of ERK1/2 has been shown to occur in response to mechanical load,^(41,42) it is conceivable that disruption of gap junctional communication may attenuate osteoblast/osteocyte ability to respond to mechanical strain, perhaps by removing a mechanism that allows cell-cell diffusion of signaling molecules and signal amplification.⁽³⁹⁾ It has been proposed that the osteocyte acts as the mechanosensor and communicates load induced signals to the osteoblast, through Cx43-dependent GJIC.^(43,44) Indeed, a recent study showed that osteocytic cells exposed to fluid flow can transmit signals to osteoblastic cells in direct contact but not exposed to fluid flow, resulting in increased alkaline phosphatase expression.⁽⁴⁵⁾ Because in *ColCre;Gjal*^{-flox} mice Cx43 is absent from both osteocytes and osteoblasts, dissection of the relative roles of osteocytes and osteoblasts in the Cx43-dependent anabolic response to load will require a more cell-specific gene ablation model.

Other mechanisms are possible. For example, Cx43 has been proposed as a downstream target of Wnt signaling,^(16,46) based on the finding that *Gjal* is upregulated in response to mechanical load in transgenic mice expressing the mutant *LRP5*^{G171V} allele associated with high bone mass phenotype.⁽¹⁶⁾ Importantly, anabolic response to mechanical load is absent in mice genetically deficient in *Lrp5*,⁽⁴⁷⁾ and it would be interesting to determine whether Cx43 and Wnt/ β -catenin signaling are on the same osteogenic pathway activated by mechanical stimuli.

In summary, we showed that the *ColCre;Gjal*^{-flox} mice have larger but thinner long bones and exhibit attenuated activation of new bone formation to mechanical loading. Therefore, these results further support the notion that Cx43 is involved in adaptive response of bone forming cells to a variety of anabolic stimuli.

ACKNOWLEDGMENTS

This work was supported by NIH Grant AR041255 and supplement (RC) and AR047867 (MJS).

REFERENCES

- Goodenough DA, Goliger JA, Paul DL 1996 Connexins, connexons, and intercellular communication. *Annu Rev Biochem* **65**:475–502.
- Yeager M, Nicholson BJ 1996 Structure of gap junction intercellular channels. *Curr Opin Struct Biol* **6**:183–192.
- Civitelli R, Beyer EC, Warlow PM, Robertson AJ, Geist ST, Steinberg TH 1993 Connexin43 mediates direct intercellular communication in human osteoblastic cell networks. *J Clin Invest* **91**:1888–1896.
- Yamaguchi DT, Ma D, Lee A, Huang JT, Gruber HE 1994 Isolation and characterization of gap junctions in the osteoblastic MC3T3-E1 cell line. *J Bone Miner Res* **9**:791–803.
- Donahue HJ, McLeod KJ, Rubin CT, Andersen J, Grine EA, Hertzberg EL, Brink PR 1995 Cell-to-cell communication in osteoblastic networks: Cell line-dependent hormonal regulation of gap junction function. *J Bone Miner Res* **10**:881–889.
- Steinberg TH, Civitelli R, Geist ST, Robertson AJ, Hick E, Veenstra RD, Wang H-Z, Warlow PM, Westphale EM, Laing JG, Beyer EC 1994 Connexin43 and connexin45 form gap junctions with different molecular permeabilities in osteoblastic cells. *EMBO J* **13**:744–750.
- Lecanda F, Warlow PM, Sheikh S, Furlan F, Steinberg TH, Civitelli R 2000 Connexin43 deficiency causes delayed ossification, craniofacial abnormalities, and osteoblast dysfunction. *J Cell Biol* **151**:931–944.
- Richardson R, Donnai D, Meire F, Dixon MJ 2004 Expression of *Gjal* correlates with the phenotype observed in oculodentodigital syndrome/type III syndactyly. *J Med Genet* **41**:60–67.
- Paznekas WA, Boyadjiev SA, Shapiro RE, Daniels O, Wollnik B, Keegan CE, Innis JW, Dinulos MB, Christian C, Hannibal MC, Jabs EW 2003 Connexin 43 (GJA1) mutations cause the pleiotropic phenotype of oculodentodigital dysplasia. *Am J Hum Genet* **72**:408–418.
- Flenniken AM, Osborne LR, Anderson N, Ciliberti N, Fleming C, Gittens JE, Gong XQ, Kelsey LB, Lounsbury C, Moreno L, Nieman BJ, Peterson K, Qu D, Roscoe W, Shao Q, Tong D, Veitch GI, Voronina I, Vukobradovic I, Wood GA, Zhu Y, Zirngibl RA, Aubin JE, Bai D, Bruneau BG, Grynpas M, Henderson JE, Henkelman RM, McKerlie C, Sled JG, Stanford WL, Laird DW, Kidder GM, Adamson SL, Rossant J 2005 A *Gjal* missense mutation in a mouse model of oculodentodigital dysplasia. *Development* **132**:4375–4386.
- Dobrowolski R, Sasse P, Schrickel JW, Watkins M, Kim JS, Rackauskas M, Troatz C, Ghanem A, Tiemann K, Degen J, Bukauskas FF, Civitelli R, Lewalter T, Fleischmann BK, Willecke K 2008 The conditional connexin43G138R mouse mutant represents a new model of hereditary oculodentodigital dysplasia in humans. *Hum Mol Genet* **17**:539–554.
- Saunders MM, You J, Trosko JE, Yamasaki H, Li Z, Donahue HJ, Jacobs CR 2001 Gap junctions and fluid flow response in MC3T3-E1 cells. *Am J Physiol Cell Physiol* **281**:C1917–C1925.
- Cherian PP, Siller-Jackson AJ, Gu S, Wang X, Bonewald LF, Sprague E, Jiang JX 2005 Mechanical strain opens connexin 43 hemichannels in osteocytes: A novel mechanism for the release of prostaglandin. *Mol Biol Cell* **16**:3100–3106.
- Jørgensen NR, Henriksen Z, Brot C, Eriksen EF, Sorensen OH, Civitelli R, Steinberg TH 2000 Human osteoblastic cells

- propagate intercellular calcium signals by two different mechanisms. *J Bone Miner Res* **15**:1024–1032.
15. Ziambaras K, Lecanda F, Steinberg TH, Civitelli R 1998 Cyclic stretch enhances gap junctional communication between osteoblastic cells. *J Bone Miner Res* **13**:218–228.
 16. Robinson JA, Chatterjee-Kishore M, Yaworsky PJ, Cullen DM, Zhao W, Li C, Kharode Y, Sauter L, Babij P, Brown EL, Hill AA, Akhter MP, Johnson ML, Recker RR, Komm BS, Bex FJ 2006 Wnt/beta-catenin signaling is a normal physiological response to mechanical loading in bone. *J Biol Chem* **281**:31720–31728.
 17. Reaume AG, De Sousa PA, Kulkarni S, Langille BL, Zhu D, Davies TC, Juneja SC, Kidder GM, Rossant J 1995 Cardiac malformation in neonatal mice lacking connexin43. *Science* **267**:1831–1834.
 18. Ya J, Erdtsieck-Ernste EB, de Boer PA, van Kempen MJ, Jongma H, Gros D, Moorman AF, Lamers WH 1998 Heart defects in connexin43-deficient mice. *Circ Res* **82**:360–366.
 19. Castro CH, Stains JP, Sheikh S, Szejnfeld VL, Willecke K, Theis M, Civitelli R 2003 Development of mice with osteoblast-specific connexin43 gene deletion. *Cell Commun Adhes* **10**:445–450.
 20. Chung DJ, Castro CH, Watkins M, Stains JP, Chung MY, Szejnfeld VL, Willecke K, Theis M, Civitelli R 2006 Low peak bone mass and attenuated anabolic response to parathyroid hormone in mice with an osteoblast-specific deletion of connexin43. *J Cell Sci* **119**:4187–4198.
 21. Truett GE, Heeger P, Mynatt RL, Truett AA, Walker JA, Warman ML 2000 Preparation of PCR-quality mouse genomic DNA with hot sodium hydroxide and tris (HotSHOT). *Bio-techniques* **29**:52–54.
 22. Castro CH, Shin CS, Stains JP, Cheng SL, Sheikh S, Mbalaviele G, Szejnfeld VL, Civitelli R 2004 Targeted expression of a dominant-negative N-cadherin in vivo delays peak bone mass and increases adipogenesis. *J Cell Sci* **117**:2853–2864.
 23. Silva MJ, Brodt MD, Hucker WJ 2005 Finite element analysis of the mouse tibia: Estimating endocortical strain during three-point bending in SAMP6 osteoporotic mice. *Anat Rec Part A* **283**:380–390.
 24. Robling AG, Burr DB, Turner CH 2000 Partitioning a daily mechanical stimulus into discrete loading bouts improves the osteogenic response to loading. *J Bone Miner Res* **15**:1596–1602.
 25. Akhter MP, Cullen DM, Pedersen EA, Kimmel DB, Recker RR 1998 Bone response to in vivo mechanical loading in two breeds of mice. *Calcif Tissue Int* **63**:442–449.
 26. Chow JW, Wilson AJ, Chambers TJ, Fox SW 1998 Mechanical loading stimulates bone formation by reactivation of bone lining cells in 13-week-old rats. *J Bone Miner Res* **13**:1760–1767.
 27. Boppart MD, Kimmel DB, Yee JA, Cullen DM 1998 Time course of osteoblast appearance after in vivo mechanical loading. *Bone* **23**:409–415.
 28. Parfitt AM, Drezner MK, Glorieux FH, Kanis JA, Malluche H, Meunier PJ, Ott SM, Recker RR 1987 Bone histomorphometry: Standardization of nomenclature, symbols, and units. Report of the ASBMR Histomorphometry Nomenclature Committee. *J Bone Miner Res* **2**:595–610.
 29. Cullen DM, Smith RT, Akhter MP 2000 Time course for bone formation with long-term external mechanical loading. *J Appl Physiol* **88**:1943–1948.
 30. Martin RB, Atkinson PJ 1977 Age and sex-related changes in the structure and strength of the human femoral shaft. *J Biomech* **10**:223–231.
 31. Smith RW Jr, Walker RR 1964 Femoral expansion in aging women: Implications for osteoporosis and fractures. *Science* **145**:156–157.
 32. Koval M, Geist ST, Westphale EM, Kemendy AE, Civitelli R, Beyer EC, Steinberg TH 1995 Transfected connexin45 alters gap junction permeability in cells expressing endogenous connexin43. *J Cell Biol* **130**:987–995.
 33. Veenstra RD, Wang H-Z, Westphale EM, Beyer EC 1992 Multiple connexins confer distinct regulatory and conductance properties of gap junctions in developing heart. *Circ Res* **71**:1277–1283.
 34. Grimston SK, Screen J, Haskell JH, Chung DJ, Brodt MD, Silva MJ, Civitelli R 2006 Role of connexin43 in osteoblast response to physical load. *Ann N Y Acad Sci* **1068**:214–224.
 35. Turner CH, Forwood MR, Rho JY, Yoshikawa T 1994 Mechanical loading thresholds for lamellar and woven bone formation. *J Bone Miner Res* **9**:87–97.
 36. Wergedal JE, Sheng MH, Ackert-Bicknell CL, Beamer WG, Baylink DJ 2005 Genetic variation in femur extrinsic strength in 29 different inbred strains of mice is dependent on variations in femur cross-sectional geometry and bone density. *Bone* **36**:111–122.
 37. Kodama Y, Umemura Y, Nagasawa S, Beamer WG, Donahue LR, Rosen CR, Baylink DJ, Farley JR 2000 Exercise and mechanical loading increase periosteal bone formation and whole bone strength in C57BL/6J mice but not in C3H/HeJ mice. *Calcif Tissue Int* **66**:298–306.
 38. Judex S, Donahue LR, Rubin C 2002 Genetic predisposition to low bone mass is paralleled by an enhanced sensitivity to signals anabolic to the skeleton. *FASEB J* **16**:1280–1282.
 39. Stains JP, Civitelli R 2005 Gap junctions regulate extracellular signal-regulated kinase signaling to affect gene transcription. *Mol Biol Cell* **16**:64–72.
 40. Stains JP, Lecanda F, Screen J, Towler DA, Civitelli R 2003 Gap junctional communication modulates gene transcription by altering the recruitment of Sp1 and Sp3 to connexin-response elements in osteoblast promoters. *J Biol Chem* **278**:24377–24387.
 41. Jessop HL, Rawlinson SC, Pitsillides AA, Lanyon LE 2002 Mechanical strain and fluid movement both activate extracellular regulated kinase (ERK) in osteoblast-like cells but via different signaling pathways. *Bone* **31**:186–194.
 42. Plotkin LI, Mathov I, Aguirre JI, Parfitt AM, Manolagas SC, Bellido T 2005 Mechanical stimulation prevents osteocyte apoptosis: Requirement of integrins, Src kinases, and ERKs. *Am J Physiol Cell Physiol* **289**:C633–C643.
 43. Duncan RL, Turner CH 1995 Mechanotransduction and the functional response of bone to mechanical strain. *Calcif Tissue Int* **57**:344–358.
 44. Donahue HJ 2000 Gap junctions and biophysical regulation of bone cell differentiation. *Bone* **26**:417–422.
 45. Taylor AF, Saunders MM, Shingle DL, Cimbala JM, Zhou Z, Donahue HJ 2007 Mechanically stimulated osteocytes regulate osteoblastic activity via gap junctions. *Am J Physiol Cell Physiol* **292**:C545–C552.
 46. van der Heyden MA, Rook MB, Hermans MM, Rijksen G, Boonstra J, Defize LH, Destree OH 1998 Identification of connexin43 as a functional target for Wnt signalling. *J Cell Sci* **111**:1741–1749.
 47. Sawakami K, Robling AG, Ai M, Pitner ND, Liu D, Warden SJ, Li J, Maye P, Rowe DW, Duncan RL, Warman ML, Turner CH 2006 The Wnt co-receptor LRP5 is essential for skeletal mechanotransduction but not for the anabolic bone response to parathyroid hormone treatment. *J Biol Chem* **281**:23698–23711.

Address reprint requests to:

Susan K Grimston, PhD
 Division of Bone and Mineral Diseases
 Washington University in St Louis
 4940 Parkview Pl., Campus Box 8301
 St Louis, MO 63110, USA
 E-mail: Sgrimsto@im.wustl.edu

Received in original form August 1, 2007; revised form February 12, 2008; accepted February 15, 2008.